Lost Alpha Faraday Cup Foil Noise Characterization During Joint European Torus Plasma Post-Processing Analysis

P. J. Bonofiglo,[1, a)] V. Kiptily,[2] V. Goloborodko,[3] Ž. Štancar,[2, 4] M. Podestà,[1] F. E. Cecil,[5] C. D. Challis,[2] J. Hobirk,[6] A. Kappatou,[6] E. Lerche,[2, 7] I. S. Carvalho,[8] J. Garcia,[9] J. Mailloux,[2] C. F. Maggi,[2] A. G. Meigs,[2] and JET Contributors[b)]

[1)] *Princeton Plasma Physics Laboratory, Princeton, NJ, 08540 USA*
[2)] *UKAEA, CCFE, Culham Science Centre, Abingdon, Oxon, OX14 3DB, UK*
[3)] *Kyiv Institute for Nuclear Research, Prospekt Nauky 47, Kyiv, 03680, Ukraine*
[4)] *Jožef Stefan Institute, Jamova 39, SI-1000 Ljubljana, Slovenia*
[5)] *Colorado School of Mines, Golden, CO, 80401, USA*
[6)] *Max-Planck-Institut für Plasmaphysik, D-85748 Garching, Germany*
[7)] *LPP-ERM-KMS, Association EUROFUSION-Belgian State, TEC Partner, B-1000 Brussels, Belgium*
[8)] *Instituto de Plasmas e Fusão Nuclear, Instituto Superior Técnico, Universidade de Lisboa, 1049-001 Lisbon, Portugal*
[9)] *CEA-IRFM, F-13108 Saint Paul Lez Durance, France*

(Dated: 17 August 2022)

Capacitive plasma pickup is a well-known and difficult problem for plasma-facing edge diagnostics. This problem must be addressed to ensure an accurate and robust interpretation of the real signal measurements versus noise. The Joint European Torus' (JET) Faraday cup fast ion loss detector array is particularly prone to this issue and can be used as a testbed to prototype solutions. The separation and distinction between warranted fast ion signal and electromagnetic plasma noise has traditionally been solved with hardware modifications, but a more versatile post-processing approach is of great interest. This work presents post-processing techniques to characterize the signal noise. While hardware changes and advancements may be limited, the combination with post-processing procedures allows for more rapid and robust analysis of measurements. The characterization of plasma pickup noise is examined for alpha losses in a discharge from JET's tritium campaign. In addition to highlighting the post-processing methodology, the spatial sensitivity of the detector array is also examined which presents significant advantages for the physical interpretation of fast ion losses.

I. INTRODUCTION

With the Joint European Torus' (JET) recent 2021 tritium and deuterium-tritium campaigns, energetic alpha particle experiments in confinement, heating, mode destabilzation, and transport studies have found a resurgence.[1] One of the key measurements from these studies is that of fast ion losses. Fast ion loss detectors (FILDs) have become ubiqutous in magnetic confinement experiments.[2–5]

JET contains an array of Faraday cup FILDs which poloidally span the outboard side of the machine from near the midplane to approximately the divertor region.[6] The Faraday cups are pre-assembled into five "pylons" which may house up to three cups across a small radial extent. This design covers a broad region and can provide spatial information on the fast ion loss footprints. Each Faraday cup is composed of four alternating layers of thin nickel foil and insulating mica which can provide a rough energy resolution for a given incident lost ion. A full description and image of the entire diagnostic array can be found in references [6] and [7].

JET's Faraday cup FILD array has been shown to suffer from strong capacitive coupling with the thermal plasma.[7,8] Based on previous campaigns and experimentation, altering the plasma conditions does not have a significant impact on altering the coupling. When any MHD is present, the foils react strongly to it and differentiating any resonant fast ion losses becomes impossible. This problem may be remedied with hardware solutions (e.g. install a grounded front-foil or build a "dummy" Faraday cup for differential analysis), but hardware modifications complicate the diagnostic design and require machine access. In addition to extended experimental campaigns, the radiological hazard imposed by tritium fuel limits personnel access and hardware changes. This was the case for JET's recent tritium and deuterium-tritium campaigns where no diagnostic modifications could be made. Therefore, it is advantageous to seek a purely post-processing approach to filter and mitigate any Faraday cup noise.

This paper discusses a general methodology for obtaining refined energetic particle loss measurements from JET's Faraday cup FILD array while accounting for capacitive plasma pickup during post-shot analysis. The FILD signals are post-processed from their original form by utilizing spectral methods and a new corrective foil signal. The approach is discussed in Section II and applied to a JET tritium discharge in Section III. The manuscript will conclude by considering the efficacy of

[a)] The author to whom correspondence may be addressed: pbonofig@pppl.gov
[b)] See author list of J. Mailloux 2022 Nucl. Fusion, doi:10.1088/1741-4326/ac47b4

the post-processing analysis method.

II. POST-PROCESSING METHODOLOGY

The analysis procedure focuses on low frequency magnetohydrodynamic (MHD) modes which have been shown to exhibit strong losses in the Faraday cup array.[7] In particular, modes which can be spectrally decomposed in frequency-space as a function of time support more sophisticated analysis techniques.

Figure 1 presents the external heating powers and a magnetic spectrogram for JET discharge 99151 from the recent tritium campaign (I_p=2.3 MA, B_0=3.4 T, n_e=7x10^{19} m^{-3}, T_e=8.5 keV). The shot is 95% tritium with a small fraction of hydrogen for minority RF-heating and residual deuterium. The neutral beams are fueled with tritium resulting in TT beam-thermal fusion reactions. The edge magnetic coil shows a variety of MHD ac-

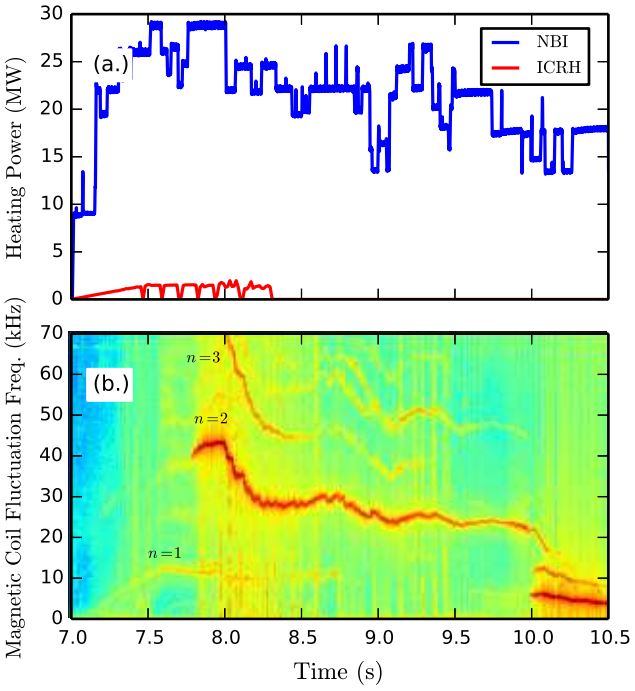

FIG. 1. External heating power, (a.), and a spectrogram from an edge magnetic Mirnov coil, (b.) for JET tritium discharge 99151. The toroidal mode numbers, n=1-3, are identifited in subplot (b.) for the observed modes.

tivity at varying frequencies and toroidal mode numbers, n, throughout the sustained heating period. Energetic ions can resonantly interact with these modes, undergo transport, and be lost. These losses are measureable with JET's fast ion loss detectors.

Figure 2 displays the spectrograms produced from one of JET's Faraday cup FILD foils and scintillator probe FILD[9] photomultiplier tubes (PMTs). The Faraday foil is taken from the pylon closest to the midplane, third radial cup (closest to the wall), and fourth (deepest) foil within the foil stack. The scintillator PMT corresponds

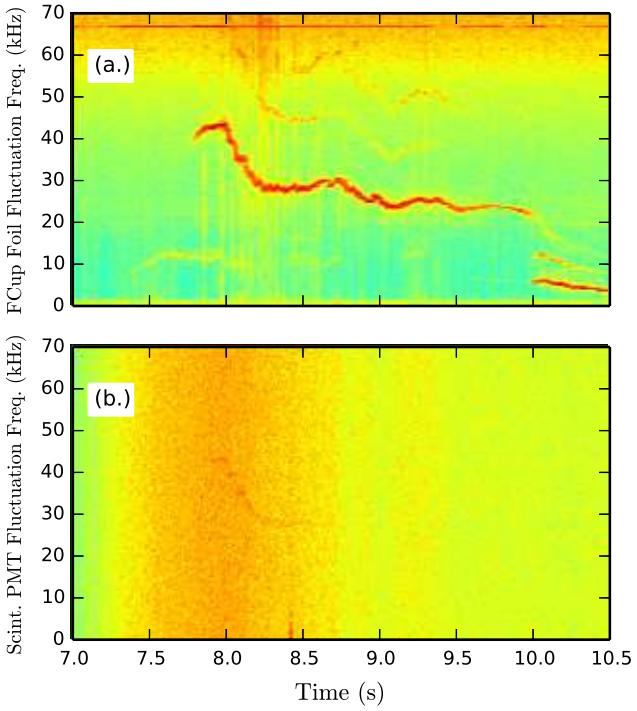

FIG. 2. Measured spectrogram signals from Faraday cup FILD foil 134 (first pylon, third radial cup, fourth foil), (a.), and PMT 10 from the scintillator probe FILD, (b.).

to a region high in gyroradius ($\sim 7-10$ cm) which correlates to order MeV energy alphas or tritons and low pitch ($cos^{-1}(v_\parallel/v) \sim 40-60°$). The magnetic features shown in 1 (b.) are clearly evident in the Faraday foil. Since the various modes can capactively couple to the foil stack, the signal shown is most-likely a combination of actual fast ion losses and plasma coupling noise. Scintillator probe FILDs, however, do not suffer from the anomalous currents that Faraday cup FILDs do and may serve to confirm the presence of lost energetic particles. The scintillator probe FILD signal in subplot (b.) shows fast ion losses coherent with the $n=2$ mode from about 7.8-8.5s and confirms that the signal detected in the Faraday foils is indeed composed of some fraction of loss energetic ions.

Since the $n=2$ mode exhibits losses, it would be beneficial to isolate this mode feature from the total Faraday foil signal. Many feature finding tools exist to find distinct features within spectrograms with varying degrees of sophistication.[10] For the purposes of this work, it is almost always possible to find at least one Faraday foil (there are a total of 44) with relatively clean features and reduced spectral noise such as Figure 2 (b.). The $n=2$ mode can easily be extracted by specifying a threshold amplitude value within a given time and frequency.

Figure 3 displays the $n=2$ mode feature shown in Figure 2 found from the Faraday foil signal in subplot (a.). The mode is highlighted in red and denotes the corresponding frequencies as a function of time that translate to a coherence with the $n=2$ mode. The mode's time and frequency variation is well captured. The Faraday

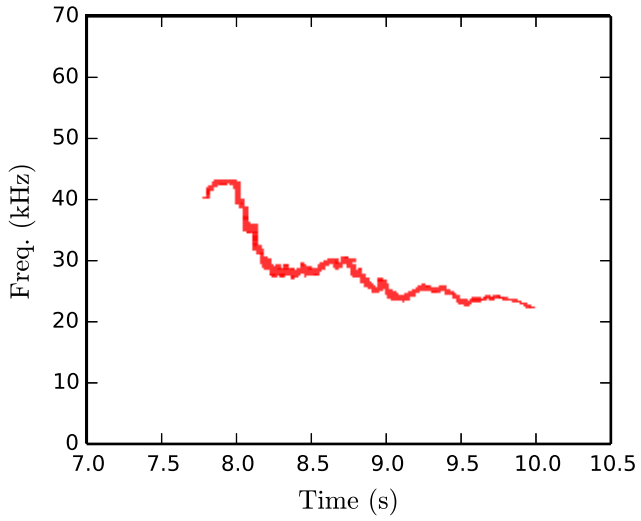

FIG. 3. The $n = 2$ mode feature extracted from the Faraday cup foil spectrogram shown in Figure 2 (a.).

foils are all digitized at the same rate, so that the foil spectrograms can be produced with the same rolling window size. This ensures that once the location of the mode feature is found from any of the foils, then the extracted structure can be used on all of the foils. This assumes that all foils have a similar response to the mode. In general, this is true since any mode-resonant losses will be coherent with the mode and exhibit the same spectral shape. Any loss differences between the cups and foils will translate to a difference in intensity within the isolated domain. Once the coherent signal for any given mode is found, any other modes present, both coherent and non-coherent, can simply be ignored. This narrows the analysis, and measured signal, down to a specific mode of interest.

Once the loss mechanism (i.e. the $n = 2$ mode) has been identified and located in frequency space, then the signal and noise need to be deconstructed. In previous work, the front-most plasma facing foil was used to correct foils deeper within a respective stack.[7] The underlying assumption was that the front-most foil would experience the strongest plasma coupling, so subtracting the front foil signal from deeper foils would remove the strongest noise components. Meaurements under vacuum showed that the foil-to-foil capacitance remained consistent across Faraday cups at a few pF, so the equal subtraction across all foils was deemed acceptable. This procedure will also discount real fast ion loss signal which may be appreciable in the front foil loss populations and overcorrect when taking the difference.

Instead, focus is placed on the deepest Faraday foil within the stack which captures higher energy ions. The deepest foil (fourth Ni layer) is susceptible to 5.6-6.35 MeV alphas, 2.0-2.25 MeV tritons, 1.45-1.65 MeV protons, and 1.78-2.0 MeV deuterons. These are relatively high energies even for energetic particles. The required ion energies are much greater than the beam injection energy (∼100 keV) and represents a small fraction of any RF-heated tail ions. Likewise, the needed alpha particle energy is much higher than the distribution created from typical TT or DT fusion. For DD interactions, the fourth foil is receptive to the slowing of the 3 MeV protons which could be appreciable in number and complicates this approach.

Tritons can be accelerated by 3rd harmonic ICRH heating and produce a continuous alpha energy spectrum from TT-fusion reactions in addition to 3.5 MeV alpha particles from residual DT interactions. Figure 4 presents the normalized alpha particle distribution as a function of energy calculated from TRANSP/NUBEAM[11] at t=8.1s for pulse 99151. The distribution peaks around 500 keV

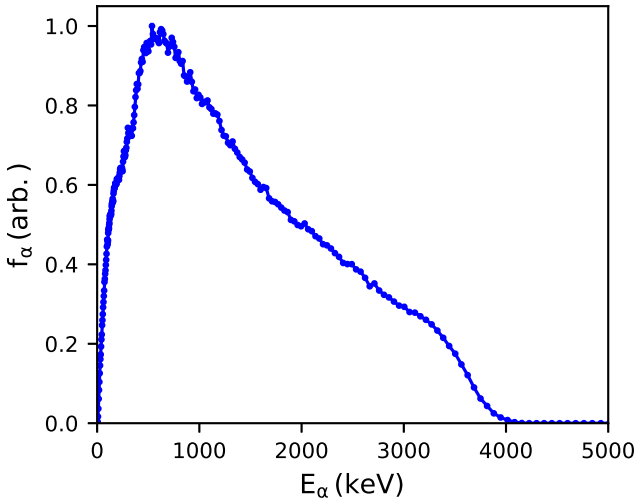

FIG. 4. The normalized alpha energy distribution as computed from TRANSP for JET shot 99151 at 8.1s.

and falls off for higher energies which is common of slowing fusion products and is in good agreement with nuclear database tables.[12] The distribution clearly approches zero for alpha energies above 5 MeV.

Since the fourth Faraday cup foil is only capable of measuring 5.6-6.35 MeV alpha particles, it can be safely assumed that this foil should be absent of any lost alpha particle signal. Therefore, any remaining lost ion signal can only come from 2.0-2.25 MeV tritons. The NUBEAM[13] and TORIC[14] codes model the RF-heating effect but often require a substantial number of statistics to model the RF-tail out to energies in excess of 1 MeV.[15] Functional forms for the RF heating distribution function decrease exponentially with energy.[16] As such, any actual lost triton signal to the fourth foil can be taken as small and negligible in regards to both fusion products and RF-heated ions.

The assumptions made in the previous paragraph may not always hold. In advanced heating scenarios, alpha populations at high energies, 4-6 MeV, exist.[17] Alfvén eigenmodes can be destabilized in JET plasmas with RF heating as well, so a super-Alfvénic RF-tail population

is at least present.[18] While the fourth foil may contain some real fast ion loss signal, the loss populations are often orders of magntiude less than those present in the first foil which is susceptible to beam losses and slowing populations.

In summary, after a discharge occurs and a mode of interest is determined with a visible presence on the Faraday foils, the mode feature is extracted in frequency and time space. This domain specifies the mode resonant losses. The deepest foil is then used as a corrective factor against the other foils within a respective stack. The mode feature domain of the fourth foil is subtracted against the same domain within the other foils, and the final signal is integrated to achieve the net fast ion loss current. This procedure is then repeated for all foils in a respective Faraday cup.

III. RESULTS

The procedure outlined in Section II was applied to JET discharge 99151 for the observed $n = 2$ mode highlighted in Figure 3. Figure 5 presents the integrated foil currents for the Faraday cup at the topmost pylon and radial cup closest to the wall. The signals are shown using

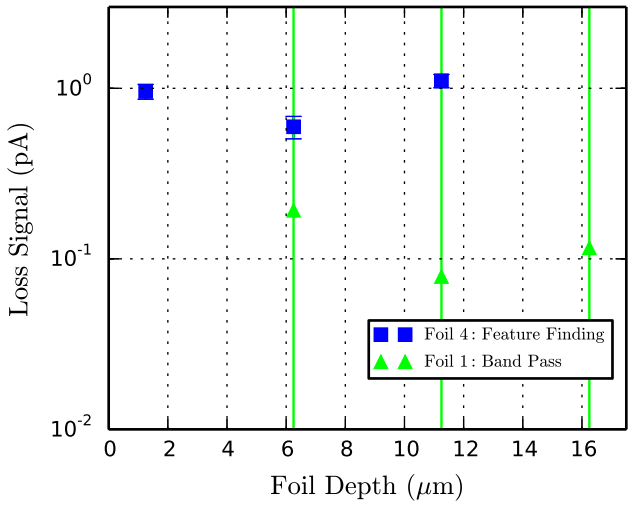

FIG. 5. Foil currents for the pylon closest to the midplane and radial cup closest to the wall for JET pulse 99151 as a function of foil depth. Blue squares represent the spectral feature method with fourth foil correction while green triangles denote the band-pass filtering method with first foil correction.

two post-processing methodologies: utilizing the $n = 2$ spectral feature in Figure 3 and subtracting the fourth foil signal from all foils (blue squares) and band-pass filtering around the $n = 2$ mode from 20-50 kHz and subtracting the first foil signal from all foils (green triangles). The error bars for the band-pass filtering method were calculated as the standard deviation, σ, within the time window of the $n = 2$ mode while the error for the spectral feature method was taken as the standard deviation of the mean, $\sigma/\sqrt{N}$, where N denotes the number of (frequency,time) bins within the feature. The standard deviation of the mean was used to account for increased uncertainty for small features (low N).

The error bars on the old method of band-pass filtering and subtracting the front foil are very large. Simply smoothing and applying a band-pass filter is too crude and does not easily acccount for the varied temporal dynamics evident. The feature finding method exactly captures the mode evolution and completely eliminates other coherent and non-coherent signal components. This reduces the error bars greatly. The individual foil signals are quite small, pA scale, because so much of the measured components are thrown out with both techniques, so the removal of noise and error bar reduction is critical.

Examining the spatial dependence, poloidally and radially, provides further insights to the two methodologies. The cumulative signal as a function of poloidal angle below the midplane, i.e pylon, is plotted in Figure 6. The

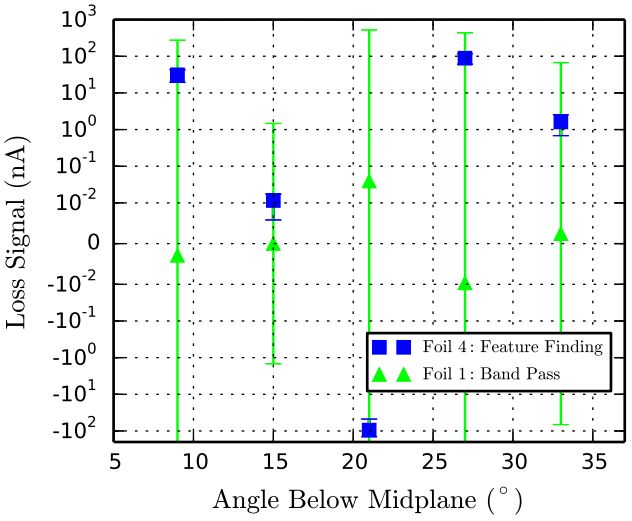

FIG. 6. Foil currents as a function of poloidal angle below the midplane (pylon) for pulse 99151. Blue squares represent the spectral feature method with fourth foil correction while green triangles denote the bandd-pass filtering method with first foil correction.

large uncertainties are still present with the band-pass filtering method. Many of the foil 1 corrected signals are also below zero which indicates that subtracting the foil 1 signal is overcorrecting the noise and eliminating any real loss signature. Thus, the corrected values are near zero, often negative, and contain large error. The high energy dependency of foil 4, however, mitigates any overcompensation of real loss signal while maintaining a good measure of the capacitive pickup. Still, singular bad foils can spoil the analysis. The Foil 4 case at 21° exhibits an unusually strong fourth foil signal and overcorrection which places the integrity of some foils into question.

The radial distribution of losses for the fourth pylon (27° below the midplane) is shown in Figure 7. For reference, the fourth pylon is located at $\sim R = 3.8$ m and each cup is about 2.5 cm apart. Again, the front-foil subtrac-

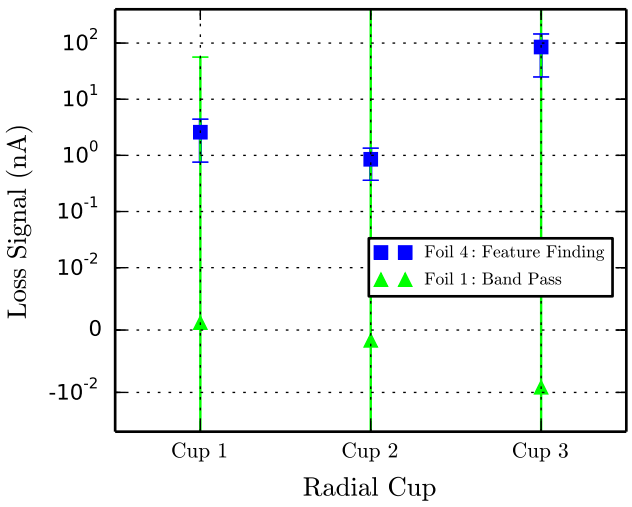

FIG. 7. Foil currents as a function of radial Faraday cup for pylon 4 (27° below the midplane) for pulse 99151. Blue squares represent the spectral feature method with fourth foil correction while green triangles denote the band-pass filtering method with first foil correction.

tion leads to an overcorrection. The new feature finding method shows total cup signals at about 1-90 nA which is in good agreement with estimated losses.

The neutron rate is used as a proxy for alpha particle production. Integrating over the $n = 2$ mode existence gives a total of $\sim 1.9\times10^{19}$ neutrons. The areal fraction of the detector (A_{FILD}/A_{wall} where A_{FILD} is the total aperture area and A_{wall} is the total vessel wall area) is about 5.42×10^{-6}. Assuming isotropic losses on the vessel wall (not entirely true based on the particle transport at hand) and a reasonable loss fraction of 2-10%, gives a total loss current of 640-3200 nA or 40-210 nA per Faraday cup assuming an even distribution among the cups. These values likely serve as maximums considering this assumes an even loss distribution, the actual areal fraction is most likely lower, and non-coherent losses are discarded. Thus, Figures 6 and 7 demonstrate that the actual loss fraction is around a few percent. Unlike the band-pass filtering approach, the new methodolgy outlined in Section II gives a reasonable estimate of losses with experiment. Additionally, the new approach better highlights poloidal and radial variation which could have important physical meaning and elucidate new transport mechanics.

IV. CONCLUSION

A methodolgy was proposed for better characterizing and correcting the capacitive plasma pickup noise in JET's Faraday cup lost alpha detector array. Mode resonant losses can be extracted from the Faraday foil spectrograms to give a more exact description of losses in (frequency,time)-space. The deepest foil within a given Faraday stack is subtracted from the others as a noise correction. The fourth foil maintains the capacitive plasma pickup signature while minimizing real lost particle signal. Utilizing this new post-processing methodology, one finds that the measurement uncertainty is greatly reduced while more accurate lost ion signal values are obtained.

Some key assumptions are made in the post-processing analysis. Namely, that the capacitiive pickup among foils is approximately consistent among all foils in a stack, and that the real losses on the fourth foil are negligible. Exactly knowing the loss population would require verification of the energetic particle distribution function and its associated losses. This is a challenging task that requires detailed modeling so is not always pertinent when analyzing a large number of discharges. Obtaining a measurement of the exact plasma coupling is even harder and would require detailed modelling of the edge electric field. Additionally, the spectral feature finding method does not account for non-coherent losses. Therefore, hardware changes still remain the best path forward for mitigating the plasma capacitive pickup. However, as machine access is limited and diagnostic upgrades occur infrequently, the bulk of noise characterization and correction must be done during post-processing analysis.

ACKNOWLEDGEMENTS

This manuscript is based upon work supported by the U.S. Department of Energy, Office of Science, Office of Fusion Energy Sciences, and has been authored by Princeton University under Contract Number DE-AC02-09CH11466 with the U.S. Department of Energy. This work has been carried out within the framework of the EUROfusion Consortium, funded by the European Union via the Euratom research and training programme (Grant Agreement No 101052200 - Eurofusion). Views and opinions expressed are however those of the author(s) only and do not necessarily reflect those of the European Union or the European Commission. Neither the European Union nor the European Commission can be held responsible for them.

DATA AVAILABILITY STATEMENT

The data that support the findings of this study are available from the corresponding author upon reasonable request.

[1] J. Mailloux *et al.*, Nucl. Fusion , 042026 (2022).
[2] M. Garcia-Munoz *et al.*, Rev. Sci. Instrum. **80**, 053503 (2009).
[3] M. Garcia-Munoz *et al.*, Rev. Sci. Instrum. **87**, 11D829 (2016).
[4] A. Werner *et al.*, Rev. Sci. Instrum. **72**, 780 (2001).
[5] D. Kulla *et al.*, Plasma Phys. Control. Fusion **64**, 035006 (2022).
[6] D. S. Darrow *et al.*, Rev. Sci. Instrum. **75**, 3566 (2004).
[7] P. J. Bonofiglo *et al.*, Rev. Sci. Instrum. **91**, 093502 (2020).
[8] F. E. Cecil *et al.*, Rev. Sci. Instrum. **81**, 10D326 (2010).
[9] S. Baeumel *et al.*, Rev. Sci. Instrum. **75**, 3563 (2004).
[10] D. R. Ferreira *et al.*, Mach. Learn: Sci. Technol. **3**, 015015 (2022).
[11] B. Joshua *et al.*, "2018 *TRANSP Software* USDOE Office of Science (SC), Fusion Energy Sciences (FES) (https://doi:10.11578/dc.20180627.4),".
[12] www-nds.iaea.org/.
[13] A. Pankin *et al.*, Commput. Phys. Commun. **159**, 157 (2004).
[14] M. Brambilla *et al.*, Plasma Phys. Control Fusion **41**, 1 (1999).
[15] P. J. Bonofiglo *et al.*, Nucl. Fusion **62**, 026026 (2022).
[16] C. Di Troia, Plasma Phys. Control. Fusion **54**, 105017 (2012).

[17]V. G. Kiptily *et al.*, Plasma Phys. Control. Fusion **64**, 064001 (2022).

[18]A. Fasoli *et al.*, Nucl. Fusion **36**, 258 (1996).